

# Engineering Notes

ENGINEERING NOTES are short manuscripts describing new developments or important results of a preliminary nature. These Notes should not exceed 2500 words (where a figure or table counts as 200 words). Following informal review by the Editors, they may be published within a few months of the date of receipt. Style requirements are the same as for regular contributions (see inside back cover).

## Coupled Aerodynamic/Structural Optimization of a Subsonic Transport Wing Using a Surrogate Model

Ke-shi Zhang,\* Zhong-hua Han,<sup>†</sup> Wei-ji Li,<sup>‡</sup> and Wen-ping Song<sup>§</sup>

Northwestern Polytechnical University,  
710072 Xi'an, People's Republic of China

DOI: 10.2514/1.36047

### I. Introduction

IN RECENT years, surrogate-model-based multidisciplinary design optimization (MDO) has received increased attention in the design optimization of complex three-dimensional wing and aircraft configurations. An optimal joined-wing configuration was presented based on the response-surface method (RSM) [1]. Considering the aeroelastic effect, MSC.FlightLoads was used to compute aerodynamic distributions, and MSC.Nastran was used to analyze structural performance. Multidisciplinary multipoint design optimization for the supersonic fighter wing was also performed based on RSM [2]. The coupled aerodynamic and structural optimization of an ONERA M6 wing was carried out with computational fluid dynamics (CFD) solver KTRAN for aerodynamic analysis and MSC.Nastran for structural analysis [3]. Conceptual design of conventional and oblique wing configurations for small supersonic aircraft was implemented with high- and low-fidelity modeling integrated using a kriging model [4].

This work focuses on the MDO of a high-subsonic transport aircraft wing of a wing/body combination, considering the static aeroelastic effect. A computational technique based on the quasi-simultaneous viscous–inviscid coupling scheme is used for computing transonic flow over the wing/body combination, taking into account the viscous effects on the wing. The finite element method (FEM)-based commercial software ANSYS is used for the structural analysis. This preliminary design is a necessary first step for further complete design of aerodynamic shape and structure.

Received 4 December 2007; revision received 1 February 2008; accepted for publication 30 March 2008. Copyright © 2008 by the American Institute of Aeronautics and Astronautics, Inc. All rights reserved. Copies of this paper may be made for personal or internal use, on condition that the copier pay the \$10.00 per-copy fee to the Copyright Clearance Center, Inc., 222 Rosewood Drive, Danvers, MA 01923; include the code 0021-8669/08 \$10.00 in correspondence with the CCC.

\*Associate Professor, School of Aeronautics, P.O. Box 120, 127 West Youyi Road; zhangkeshi@nwpu.edu.cn.

<sup>†</sup>Ph.D., School of Aeronautics, P.O. Box 754, 127 West Youyi Road; hanzh@nwpu.edu.cn.

<sup>‡</sup>Professor, School of Aeronautics, P.O. Box 120, 127 West Youyi Road; lwjnwpu@126.com.

<sup>§</sup>Professor, School of Aeronautics, P.O. Box 754, 127 West Youyi Road; wpsong@nwpu.edu.cn.

### II. Descriptions of Surrogate-Model Methods

The surrogate-model method replaces the complicated and time-consuming analysis in optimization with approximation models with greater computational efficiency and nearly identical accuracy. It simplifies the integration design optimization of large and complicated engineering systems. In this work, three surrogate models are adopted: RSM [5], kriging model (KM) [6], and radial-basis function network (RBF) [7]. The uniform-design method [8] is employed to create uniform distributed sample points.

#### A. Response-Surface Method

RSM develops polynomial approximation models by fitting the sample data using a least-squares regression technique. In many RSM applications, the quadratic polynomial model provides the best compromise between modeling accuracy and computational expense out of all the linear or higher-order polynomial models. It can smooth out the various scales of numerical noise present in the data while it captures the global trend of the variation.

The quadratic polynomial approximation can be written in the following form:

$$\hat{y}(\mathbf{x}) = \beta_0 + \sum_{i=1}^{N_V} \beta_i x_i + \sum_{i=1}^{N_V} \beta_{ii} x_i^2 + \sum_{1 \leq i < j \leq N_V} \beta_{ij} x_i x_j \quad (1)$$

where  $\mathbf{x} \in R^{N_V}$ . The unknown coefficients  $\beta_0$ ,  $\beta_i$ ,  $\beta_{ii}$ , and  $\beta_{ij}$  are determined by least-squares regression, which minimizes the sum of the squares of the deviations of predicted values  $\hat{y}(\mathbf{x})$  from the actual values  $y(\mathbf{x})$ .

#### B. Kriging Model

Different from RSM, KM and RBF are both interpolating models. They are better than RSM in the case of modeling multimodel functions. As expressed in Eq. (2), KM is composed of a known approximation function  $f(\mathbf{x})$  and a Gaussian random function  $Z(\mathbf{x})$ :

$$y(\mathbf{x}) = f(\mathbf{x}) + Z(\mathbf{x}) \quad (2)$$

The  $f(\mathbf{x})$  function is a global model for the entire design space based on a series of response observations; it is sometimes taken as a constant. In this study, we employ the quadratic response-surface model. The  $Z(\mathbf{x})$  function creates a localized deviation from the global model so that the kriging model interpolates the  $N_S$  sample data points, which is a realization of the stochastic process with mean zero, variance  $\sigma^2$ , and nonzero covariance.

#### C. Radial-Basis Function Network

Among all kinds of neural networks, RBF is commonly selected to create approximation models due to its better attribute in this aspect. RBF takes radial-basis function as a transfer function of the neural network. The predicted estimate  $\hat{y}(\mathbf{x})$  of the response  $y(\mathbf{x})$  at untried value  $\mathbf{x}$  is given by

$$\hat{y}(\mathbf{x}) = \sum_{p=1}^P \hat{\lambda}_p \varphi_p(\mathbf{x}) + \hat{\theta}, \quad \mathbf{x} \in R^{N_V} \quad (3)$$

where  $P$  is the number of hidden layers;  $\varphi_p$  is a radial-basis function acting as the transfer function of the  $p$ th hidden layer, and  $\lambda_p$  is its

weighting coefficient; and  $\theta$  is an unknown value. The unknown parameters in  $\varphi_p$  should be computed based on sample data points. Then the unknown coefficients  $\hat{\lambda}_p$  and  $\hat{\theta}$  can be calculated by least-squares estimation.

### III. Analysis Model

#### A. Aerodynamic Analysis

A computational technique based on the quasi-simultaneous viscous–inviscid coupling scheme is employed for computing transonic flow over a wing/body combination, taking into account the viscous effect on the wing. An external flow is calculated with the account of the expected boundary-layer response. The using of the quasi-simultaneous coupling ensures the effective and rapid computation of viscous–inviscid interaction, including a moderate separation regime. The viscous wake effects are also taken into consideration. The laminar and turbulent compressible three-dimensional boundary layer is computed by a finite difference method. The calculation of the external flow is carried out on the basis of numerical integration of the conservative full potential equation. (The detail of the method can be also found in [9]). The configuration of the wing/body combination is shown in Fig. 1.

#### B. Structural Analysis

The FEM-based commercial software ANSYS is used for analyzing the structural performance of the wing with a double-beam sandwich structure. The analysis is programmed with APDL language. Spars are arranged at 20 and 70% chordwise locations. For simplicity, the flanges of the spar and the stringers are combined with upper and lower skins as the integral wallboard structure, as done in [2]. The structural-analysis model consists of 300,000 elements. It takes about 5 min to perform each finite element analysis of the wing structure. The characteristics of the finite elements of upper skin, lower skin, rib webs, and spar webs are that the element type is Shell63 and the material is aluminum alloy LY12. Shell63 has both bending and membrane capabilities. Both in-plane and normal loads are permitted. The element has 6 degrees of freedom at each node.

#### C. Aeroelastic Analysis

Unlike fighter wings with low aspect ratios, the aspect ratio of the transport aircraft wing is so high that aeroelastic deformation of the wing is very apparent. Hence, iteration of static aeroelastic analysis is performed for the aerodynamic/structural optimization of the high-subsonic transport aircraft wing. A weak-coupling method is adopted for static aeroelastic analysis. In this work, aeroelastic analysis usually converges after 5–10 iterations. The different mesh used in aerodynamic and structural analysis causes the difficulty in aeroelastic analysis. In this study, reasonable simplification is made for the difficulty. Because the major deformation of the wing is due to bending and torsional behavior, it is assumed that only the translations of airfoil and rotations of the airfoil about the  $z$  axis are considered to create a new CFD mesh. The translation deformation

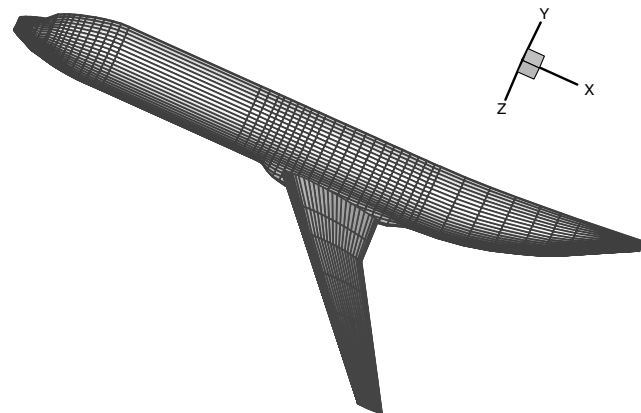


Fig. 1 Configuration of the wing/body combination.

Table 1 Definition of design variables

| Design variable                             | Lower limit | Upper limit |
|---|-------------|-------------|
| Span $B$ , m                                | 26          | 34          |
| Taper ratio $\lambda$                       | 0.2         | 0.4         |
| Linear twist angle $\theta$ , deg           | −3          | −1          |
| Sweep angle on leading edge $\Lambda$ , deg | 25          | 35          |
| Thickness of front-spar web $T_{FS}$ , mm   | 2           | 6           |
| Thickness of back-spar web $T_{BS}$ , mm    | 2           | 6           |
| Thickness of lower skin $T_{LS}$ , mm       | 3           | 7           |
| Thickness of upper skin $T_{US}$ , mm       | 3           | 7           |

along the  $z$  axis is represented by the average deformation of all the points on the airfoil.

### IV. Wing Design Problem Formulation

This work aims to perform the preliminary design for a high-subsonic transport aircraft wing of a wing/body combination. The optimization objectives are to maximize the aircraft lift-to-drag ratio and minimize the weight of the wing for a fixed maximum takeoff weight of 54 t and cruise Mach number of 0.76 at a height of 10,000 m. The wing is composed of an inner and an outer wing. The reference area of the wing is 105 m<sup>2</sup>. Eight supercritical airfoils are configured along the span. The lift should be enough to balance the weight of the aircraft, and so it is no less than 54 t. The change of wing area is limited to 5 m<sup>2</sup>. The wing must satisfy the constraints of ultimate strength and maximum deformation. The mathematical model of the wing optimization is defined as

$$\begin{aligned}
 &\max L/D \\
 &\min W_{\text{wing}} \\
 &\text{subject to } L \geq 54 \cdot 10^3 \text{ kg} \\
 &100 \leq S_{\text{wing}} \leq 110 \text{ m}^2 \\
 &\sigma_{\max} \leq \sigma_b \cdot 10^9 \text{ Pa} \\
 &\delta_{\max} \leq 1 \text{ m}
 \end{aligned} \tag{4}$$

The span, taper ratio, sweep angle, and linear twist angle are chosen as design variables that define the aerodynamic configuration of the wing. And another four variables representing the thickness of the spars and skin are selected as the design variables for the structural discipline. The definitions for the limits of the design variables are listed in Table 1.

Uniform-design table  $U_{100}(10^8)$  created 100 candidate wings for establishing the approximation-analysis models. Another 45 candidate wings are created by uniform-design table  $U_{45}(10^8)$  for evaluating the modeling accuracy. For each wing, the aeroelastic analysis is performed to obtain the responses of  $L$ ,  $L/D$ ,  $S_{\text{wing}}$ ,  $\sigma_{\max}$ ,  $\delta_{\max}$ , and  $W_{\text{wing}}$ . Then the evaluation of modeling accuracy, using the mean error  $\bar{e}$  and the standard deviation of the modeling error,  $\sigma_e$ , is performed and the results are listed in Table 2. It is found that KM and RSM have comparatively high accuracy and both are more accurate than RBF. Therefore, multi-objective optimization for the supercritical wing is performed based on RSM, due to its higher computational efficiency.

One of the candidate wings with better performance is selected as the initial point for optimization. The weighted-sum method and sequential quadratic programming method is employed to solve this problem. As optimization is finished, the optimum design is reanalyzed and the results are listed in Table 3, in which  $X_0$  and  $Y_0$  are the initial wing scheme and its response, respectively;  $X^*$  and  $Y^*$  are the optimum wing scheme and its actual response, respectively; and  $\hat{Y}$  is the estimate value of  $Y^*$ .

For the optimum wing scheme, the relative errors of approximation models are small, and the largest one is no more than 3%. It shows that the predicted value must be very close to the actual response. Compared with the initial wing, the weight of the

optimum wing is decreased by 20.44%, and lift-to-drag ratio is only decreased by 1.47%. It is found that the lift-to-drag ratio decreases, although we aim to maximize it.

On one hand, to maximize lift-to-drag ratio of the supercritical wing, the main focus is to minimize its wave drag and induced drag. The wave drag of the initial wing is very small in supercritical flow and can hardly be reduced further. On the other hand, the weight coefficients for two objectives are both 0.5. If the weight coefficient of the lift-to-drag ratio is increased, the drag must be further decreased; however, the weight cannot be decreased so much. For improving the synthesis performance, we make a compromise between weight and lift-to-drag ratio.

The optimization, together with the aeroelastic analysis of all candidate wings, only takes about two days on a Pentium(R) 4 CPU with 2.8 GHz. If more computers are used to calculate the performance of different candidate wings concurrently, the time needed can be further greatly reduced, which indicates that the surrogate-model method is suitable for such an engineering design problem. In this work, the optimization without considering the aeroelastic effect is also performed to investigate how large errors will be caused in this case. The results show that the lift-to-drag ratio decreases by 5.77% and lift decreases by 19.55% without considering the aeroelastic effect.

Figure 2 shows the contour of the equivalent stress of the optimal wing. It shows that the stress is larger in the location of the intersection of the inner wing and outer wing due to the inflexion. Figure 3 shows the pressure distribution of the optimal wing. It shows that the wing basically meets the design requirements of supercritical wing. A little nonsmoothness of the pressure distribution may be caused by nonuniform deformation of the skin. Figures 4 and 5 provide the convergence history of aeroelastic deformation, which

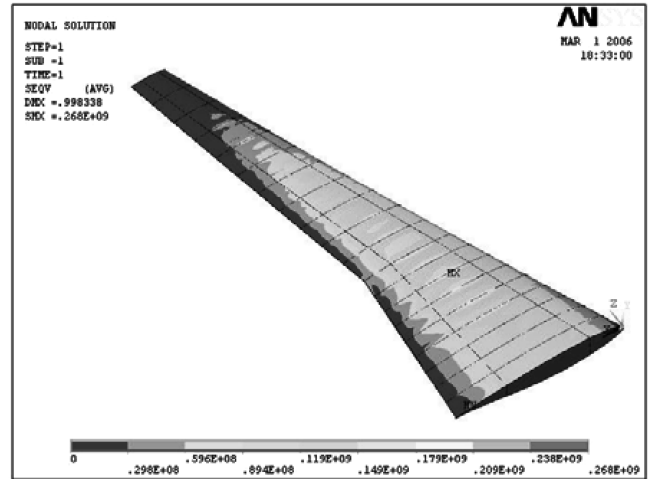


Fig. 2 Contour of equivalent stress of the optimal wing.

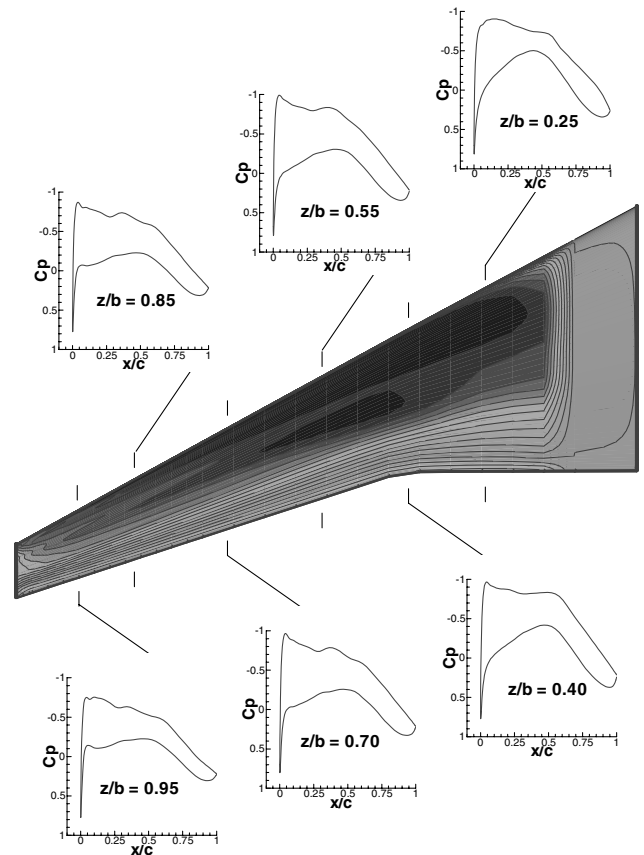


Fig. 3 Pressure distribution of the optimal wing ( $M = 0.76$ ,  $Re = 0.257E + 08$ , and  $\alpha = 0$  deg).

Table 2 Evaluation of modeling accuracy

| Parameter      | Surrogate model | $\bar{e}$ | $\sigma_e$ |
|----------------|-----------------|-----------|------------|
| $L$            | RSM             | 0.0360    | 0.0213     |
|                | KM              | 0.0362    | 0.0213     |
|                | RBF             | 0.0501    | 0.0356     |
| $L/D$          | RSM             | 0.0122    | 0.0099     |
|                | KM              | 0.0123    | 0.0097     |
|                | RBF             | 0.0231    | 0.0179     |
| $S_{wing}$     | RSM             | 0.0071    | 0.0051     |
|                | KM              | 0.0071    | 0.0051     |
|                | RBF             | 0.0096    | 0.0072     |
| $\sigma_{max}$ | RSM             | 0.0563    | 0.0535     |
|                | KM              | 0.0515    | 0.0522     |
|                | RBF             | 0.0843    | 0.0671     |
| $\delta_{max}$ | RSM             | 0.0227    | 0.0241     |
|                | KM              | 0.0227    | 0.0241     |
|                | RBF             | 0.1259    | 0.0915     |
| $W_{wing}$     | RSM             | 0.0140    | 0.0104     |
|                | KM              | 0.0142    | 0.0107     |
|                | RBF             | 0.0385    | 0.0251     |

Table 3 Optimization results when considering the aeroelastic effect

|                | $B/m$           | $\lambda$ | $\theta$ , deg     | $\Lambda$ , deg            | $T_{FS}$ , mm      | $T_{BS}$ , mm          | $T_{LS}$ , mm | $T_{US}$ , mm |
|----------------|-----------------|-----------|--------------------|----------------------------|--------------------|------------------------|---------------|---------------|
| $X^0$          | 34.00           | 0.244     | -1.667             | 29.444                     | 3.333              | 3.778                  | 6.556         | 3.889         |
| $X^*$          | 31.69           | 0.200     | -1.563             | 28.233                     | 2.232              | 2.000                  | 4.396         | 4.057         |
|                | $L$ , $10^3$ kg | $L/D$     | $S_{wing}$ , $m^2$ | $\sigma_{max}$ , $10^9$ Pa | $\delta_{max}$ , m | $W_{wing}$ , $10^3$ kg |               |               |
| $Y^0$          | 51.50           | 27.81     | 111.94             | 0.311                      | 1.191              | 3.850                  |               |               |
| $Y^*$          | 53.14           | 27.40     | 107.25             | 0.275                      | 0.991              | 3.063                  |               |               |
| $\hat{Y}$      | 54.00           | 27.45     | 106.27             | 0.267                      | 1.000              | 3.003                  |               |               |
| Modeling error | 1.61%           | 0.16%     | 0.91%              | 2.97%                      | 0.87%              | 1.85%                  |               |               |

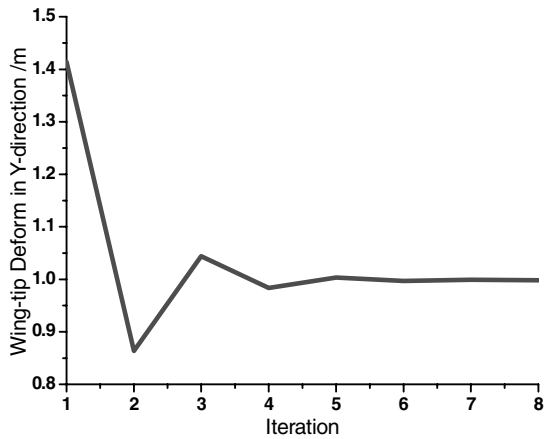


Fig. 4 Convergence history of the Y direction deform on the wing tip.

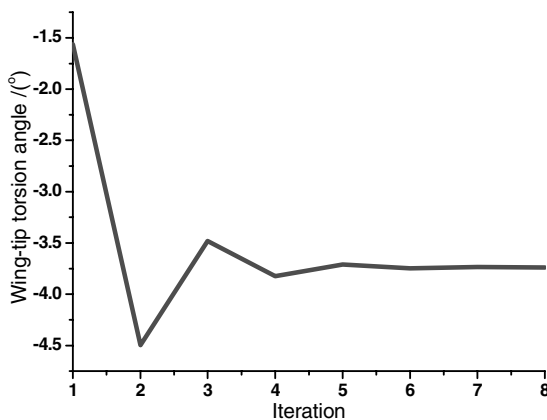


Fig. 5 Convergence history of torsional deform on the wing tip.

shows fast convergence of the aeroelastic deformation of the optimal wing.

## V. Conclusions

Coupled aerodynamic and structural optimization is performed for a high-subsonic transport aircraft wing using surrogate models. Different surrogate models (including RSM, KM, and RBF) are all used to create approximation models for six different state variables. The approximation models with the lowest modeling error are selected to replace the complicated and time-consuming analysis in optimization. Several conclusions can be made from the results. First, computation time for optimization can be greatly reduced due

to surrogate models. Second, the approximation models can reasonably predict the response, due to their low modeling error, and it is shown that KM and RSM have comparative high accuracy and both are more accurate than RBF in the current study. This indicates that surrogate-model-based MDO is applicable and makes it possible to bring detail design forward. Finally, aeroelastic properties should be taken into account, at least in the early preliminary design phase, especially for transport aircraft with high-aspect-ratio wings or large size. Not considering the aeroelastic effect will result in large errors in the design scheme.

## Acknowledgments

This research has benefited greatly from the support of the National Natural Science Foundation of China (NSFC) under grant 10702055, Ph.D. Programs Foundation of the Ministry of Education of China under grant 20070699047, and China Postdoctoral Science Foundation under grant 20070410383.

## References

- [1] Rasmussen, C. C., Canfield, R. A., and Blair, M., "Optimization Process for Configuration of Flexible Joined-wing," 10th AIAA/ISSMO Multidisciplinary Analysis and Optimization Conference, AIAA Paper 2004-4330, 2004.
- [2] Kim, Y., Lee, D. H., Kim, Y., and Yee, K., "Multidisciplinary Design Optimization of Supersonic Fighter Wing Using Response Surface Methodology," 9th AIAA/ISSMO Symposium on Multidisciplinary Analysis and Optimization, Atlanta, AIAA Paper 2002-5408, 2002.
- [3] Chen, S., Zhang, F., Renaud, G., Shi, G., and Yang, X., "A Preliminary Study of Wing Aerodynamic, Structural and Aeroelastic Design and Optimization," 9th AIAA/ISSMO Symposium on Multidisciplinary Analysis and Optimization, Atlanta, AIAA Paper 2002-5656, 2002.
- [4] Wintzer, M., Sturdza, P., and Kroo, I., "Conceptual Design of Conventional and Oblique Wing Configurations for Small Supersonic Aircraft," 44th AIAA Aerospace Sciences Meeting and Exhibit, Reno, NV, AIAA Paper 2006-930, 2006.
- [5] Giunta, A. A., "Aircraft Multidisciplinary Design Optimization Using Design of Experiments Theory and Response Surface Modeling Methods," Ph.D. Dissertation, Virginia Polytechnic Institute and State University, Blacksburg, Virginia, May, 1997.
- [6] Simpson, T. W., Mauery, T. M., Korte, J. J., and Mistree, F., "Kriging Models for Global Approximation in Simulation-Based Multidisciplinary Design Optimization," *AIAA Journal*, Vol. 39, No. 12, 2001, pp. 2233–2241. doi:10.2514/2.1234
- [7] Shankar, P., Yedavalli, R. K., and Burken, J., "An Adaptive Flight Controller Using Growing and Pruning Radial Basis Function Network," AIAA Guidance, Navigation, and Control Conference and Exhibit, AIAA Paper 2006-6415, 2006.
- [8] Fang, K. T., and Ma, C. X., *Orthogonal Design and Uniform Design*, Science Press, Beijing, 2001.
- [9] Kovalev, V. E., and Karas, O. V., "Computation of a Transonic Airfoil Flow Considering Viscous Effects and Thin Separated Regions," *La Recherche Aéronautique*, No. 1, 1991, pp. 1–15.